Author Manuscript

Diatrack particle tracking software: review of applications and performance evaluation

Pascal Vallotton[1,*], **Antoine M. van Oijen**[2], **Cynthia B. Whitchurch**[3], **Vladimir Gelfand**[4], **Leslie Yeo**[5], **Georgios Tsiavaliaris**[6], **Stephanie Heinrich**[1], **Elisa Dultz**[1], **Karsten Weis**[1], and **David Grünwald**[7]

[1]ETH Zürich, Institute of Biochemistry, Zürich, Switzerland [2]University of Wollongong, Wollongong, Australia [3]University of Technology Sydney, The ithree institute, Sydney, Australia [4]Northwestern University Feinberg School of Medicine, Department of Cell and Molecular Biology, Chicago, IL 60611, USA [5]RMIT University, Melbourne, Australia [6]Medizinische Hochschule Hannover, Hannover, Germany [7]University of Massachusetts Medical School, RNA Therapeutics Institute and Department of Biochemistry and Molecular Pharmacology, Worcester MA, USA

Abstract

Object tracking is an instrumental tool supporting studies of cellular trafficking. There are three challenges in object tracking: the identification of targets; the precise determination of their position and boundaries, and the assembly of correct trajectories. This last challenge is particularly relevant when dealing with densely populated images with low signal-to-noise ratios - conditions that are often encountered in applications such as organelle tracking, virus particle tracking, or single-molecule imaging. We have developed a set of methods that can handle a wide variety of signal complexities. They are compiled into a free software package called Diatrack. Here we review its main features and utility in a range of applications, providing a survey of the dynamic imaging field together with recommendations for effective use. The performance of our framework is shown to compare favorably to a wide selection of custom-developed algorithms, whether in terms of localization precision, processing speed, or correctness of tracks.

The last two decades have witnessed a progressive shift towards dynamic imaging as a powerful tool to learn about biological processes.[1] This shift has been supported by a panoply of technological advances, including new fluorescent proteins, precise genetic-engineering tools, and ever more powerful optical microscopes.[2] Imaging software has also played an important role in this evolution as the necessary ingredient that permits translating movies of biological phenomena into quantitative measurements suitable for statistical

*Corresponding author. ETH Zürich, Otto-Stern-Weg 3, 8093 Zurich, Switzerland, Phone: +41 (0)44 633 67 60, Fax: +41 (0)44 632 12 69, pascal.vallotton@bc.biol.ethz.ch.

analysis and data mining.[3] In particular, object tracking plays a pivotal role in investigations of e.g. vesicular traffic, cytoskeletal motions, receptor regulation, drug delivery, morphogenetic processes, or infectious mechanisms.[4] The present review describes many examples illustrating how the technique leads to accurate measurements of e.g. velocities, diffusion coefficients, turnover, processivity, or polymerization rates. While other methods, such as FRAP or FCS may lead to similar outcomes, tracking-based methods distinguish themselves as being very direct, generally applicable, and close to everyday intuition.[3,4]

The problem of faithfully following multiple targets over time has a long history, with diverse applications in air traffic control, crowd surveillance, ecology, or fluid dynamics.[5,6] Applications to biological imaging are no less diverse and include the study of membrane dynamics, bacterial motility, lineage trees, and chromosomal dynamics – each application calling for a specific tracking methodology as well as considerable custom software development efforts.[7,8]

Together with scientists from a range of application areas, we developed and made available in 2003 what was probably the first user-friendly multi-particle tracking software.[9,10] Diatrack is a versatile standalone platform for dynamic imaging built on mathematical graph algorithms, super-resolution techniques, and mathematical morphology. Its original tracking method is based on a tripartite directed graph structure that we have described previously.[11] The pressing need for tracking methods that go beyond "naïve" nearest-neighbor methodology is explained in Figure 1E, where the notion of "assignment conflict" is made clear. Briefly, associating particles identified in one image frame with those of the next frame to form correct trajectories rapidly becomes difficult as the density of particles and the amplitude of their motion increases. Because the cellular environment tends to be both very dynamic and crowded, those conditions are pervasive in biological imaging. This leads to an explosion in the number of possible associations – only one being correct. As explained in detail in[11], our graph algorithm tackles this complexity by globally and rapidly optimizing the matching of similar particles across multiple images, while still allowing particles to exceptionally appear or disappear in a balanced manner (see Figure 1E). Graph theory concepts have since then been successfully adopted by other researchers for biological object tracking.[12–14] In other fields such as particle image velocimetry, the use of graph theory for multiple particle tracking developed earlier[6], supported by classical mathematical results from the 1950s for the maximum matching between two sets of objects only.[15]

Because the task of assembling correct tracks from the sets of identified objects is largely independent from the specific nature of targets, it lies at the very heart of the tracking methodology. In order to complement this essential capability, Diatrack also provides multiple tools to identify the particles themselves. Particle "modifiers" may then optionally be activated to extract additional information from objects (for example, there is a modifier to trace the outline of the detected particles/objects). In turn, the results from these measurements may be exploited to improve the tracking outcome (for example, one may want to track only those objects that are larger than a user-defined threshold). This flexibility - allowing to very rapidly explore alternative combinations of detection methods, of modifiers, and of tracking parameters within a single integrated environment - does set Diatrack apart from a large number of tools that have been developed specifically to track a

unique type of targets, such as e.g. the tip of microtubules, a particular cell type, or single molecules[14,16].

Another important example of particle "modifier" is the refinement of particle position down to nanometer precision using sub-pixel fitting of a Gaussian-like intensity model. Diatrack exploits a robust fixed point methodology developed by Thompson et al. to achieve this goal.[17] Diatrack introduced an implementation of that method that provides super-resolution fitting in 3D, leading to performance that remains very competitive today (see e.g. Figure 2C).

Our review begins with a general overview of the software, its user interface, and its main benefits and features as summarized in Table 1. Comparing Diatrack more systematically with alternative solutions would inevitably be incomplete and reflect our imperfect knowledge of these frameworks. As an illustration of the difficulty of such an undertaking, a list of over 70 packages exclusively dedicated to the tracking of single molecules may be found under.[18]

We then turn our attention to tracking performance considerations. Because our software aims to provide a general tracking environment applicable to a diverse range of targets, one may anticipate that its performance would be sub-optimal when compared to custom-developed algorithms. Such algorithms are usually fine-tuned to follow a particular target type displaying a specific type of appearance and of motion behavior (e.g. diffusive, motor-driven, anti-parallel…).

In order to objectively assess the performance of Diatrack, we have relied on the material from a recent publication that included test data sets and results obtained by 14 participating teams.[19] One of the strengths of that material is that the tracking results were produced by the authors of the algorithms themselves so performance was not degraded by suboptimal software operation. Moreover, as a consequence of the broad call to the image analysis community that preceded the competition, many of the teams were representative of the latest technical advances in the field (for example, team 1 was the author of the well-known Mosaic tracking software while team 3 created the ICY suite; several teams have also contributed ImageJ tracking plugins that are in wide use).

Chenouard *et al.* carefully prepared image sequences in 2D and 3D that were representative of the motion and appearance of important targets in cell imaging, such as vesicles or virus particles. Multiple levels of difficulties were present in terms of density, types of motions and noise level. Because all these sequences were generated algorithmically, the exact ground truth was available (i.e. the true position of the targets as well as their true motions from frame to frame were known).

Following the presentation of the performance evaluation of Diatrack, we then review user applications, from tracking single molecules, protein foci, endosomes, nanoparticles, vesicles, speckles, and cells, to in vitro motility studies and fluid flow characterization. Because we cannot cover every application in detail, we encourage readers to consult the cited literature, the Diatrack user manual, or the authors for advice. The software may be downloaded from www.diatrack.org.

Overview of Diatrack user interface

The first tracking tools provided a powerful new approach to analyze movies of moving particles.[20] However, the command-line environment of those tools presented a significant barrier to the general user. To our knowledge, Diatrack was the first object tracking software supported by a graphical user interface—an innovation that made particle tracking generally accessible to microscopists and biologists.[9] Tracking functions - from image pre-processing to particle identification, particle selection and particle tracking -are arranged logically on the control panel, from top to bottom (see Figure 1). Other frequently used functions are readily available from toolbar buttons, including a button for super-resolution Gaussian spot fitting ⊕, for segmentation ▉ (to delineate object boundaries), and for manual removal or addition of particles ⚏. Another key innovation in Diatrack lies in the scalability, reliability, and speed of tracking, enabled by powerful graph algorithms solvers.[10,11] Because mathematical graphs can simultaneously encode all potential movements of targets, they represent natural structures to use for difficult and ambiguous tracking problems. Several dedicated graph structures were therefore introduced that, when coupled with efficient algorithms on graphs, produced excellent tracking results for biological imaging applications.

Because critical assessment of tracking results is paramount, many possibilities to visualize tracks are offered. In the default representation, the entire set of trajectories is overlaid onto the first image of the sequence (see e.g. Fig 3C). One may also overlay tracks onto a maximum intensity projection of the sequence, display tracks in 3D (the Z axis represents time, see Fig 3F), or step through the sequence one frame at a time to verify that the spots marking individual particles maintain the same color over time.

As summarized in Table 1, Diatrack offers many possibilities, not only for reliable tracking in 2D and 3D, but also in terms of track analysis and post-processing. From the set of all tracks produced, the user can retain subsets of trajectories based e.g. on object lifetime (i.e. the number of frames for which the object may be observed), velocity, entropy, diffusion coefficient etc. The user can remove any potential drift, smoothen trajectories, or close any remaining gaps in trajectories. Diatrack also allows generating plots describing the relevant dynamics quantitatively (e.g. plot track lengths, speed, diffusion coefficients, dispersion, intensity changes etc.).

Other notable features of Diatrack include options to batch process a series of TIFF image stacks or multiple AVI movies. This is particularly useful for large-scale experiments (e.g. in a screening setting) where conditions are systematically varied, resulting in gigabytes of time-lapse data.

Many possibilities are available for exporting data and plots. Entire sessions may be saved and later reloaded for further analysis. Scripting capabilities allow workflows to be automated. Entire session files may also be opened under Matlab™, and all internal variables (e.g., the variable "tracks" describing particle history, i.e. position in X, Y, and Z, successor particle, intensity, eccentricity, etc.) may be accessed and processed for more specialized analyses.

Objective performance evaluation

In recent years, the tracking field has seen an explosion in the number of algorithms and software packages. An important contribution was made by Chenouard and colleagues who put in place an extensive testing infrastructure to evaluate these activities in an objective setting, accompanied by an open competition.[19] Each participant was given one month to fine-tune his software to the difficulty of the data sets provided. There was no requirement that one should use the same software, algorithm or image analysis technique for all the different data sets.

We subjected Diatrack 3.05 to all reference data sets prepared by Chenouard et al. The tests included data of simulated vesicles, receptors, microtubule transport in 2D, and of viruses moving in 4D. In order to convey a sense for the difficulty of Chenouard's datasets, one sample is provided in the supplementary information (SuppMovie1.avi).

We compared results produced by Diatrack to the ground truth data by using the scoring tool provided (i.e. the ICY "Tracking Performance Computation" module). No modifications were made to Diatrack to perform these tasks except for the selection of appropriate image analysis parameters accessible from the GUI (i.e. the Gaussian filter width, intensity threshold, contrast threshold, and maximum particle jump allowed - only 4 parameters; all of them quite intuitive). Representative quality metrics are shown in Figure 2 (all results may be found in the supplementary information). The RMSE value reported here is a measure of the average error in particle position (lower RMSE values indicate superior performance). Alpha is a measure of the quality of the tracks themselves (larger Alpha values indicate superior performance). We refer the reader to the original publication for a description of these and other quality metrics.[19] All corresponding Diatrack session files are provided as supplementary information at http://www.diatrack.org/TrafficSI.zip (they contain the tracks produced by Diatrack and the image analysis parameters). As can be seen in Figure 2, the outcome of these tests show impressive performance for a general-purpose tracking package such as Diatrack. The software matched and even outperformed the best algorithms in a few cases.

The main area where Diatrack may need additional work is in ultra-low SNR conditions where a few custom algorithms performed better in 2D.

Selected timing information is also shown in Figure 2 panel D (an i7 4790 processor was used for Diatrack −30% faster overall than the Xeon X550 of the original publication according to: http://cpuboss.com). While Diatrack is not the fastest for 4D tracking, this was compensated by superior tracking quality results (Fig. 2, panel C). This advantage is probably due to the fact that closely adjoining targets are more easily separated in 3D. In such conditions, missed particle detections are rare and the advantage of our graph matching algorithms for trajectory assembly becomes clear.

One area of relative weakness was in the tracking of microtubule-associated particles (see supplementary information). For this dataset, targets were spatially spread-out and overlapped frequently. A dedicated method to separate these targets would be required in

order to obtain optimal performance. As our goal was only to test the Diatrack 3.05 release, we did not explore the problem further.

Object tracking workflow

The object tracking workflow is divided into two main stages: i) particle detection, and ii) trajectory assembly, where the particles detected in each frame are linked together to form complete trajectories (see Figure 1). The term "object" is used to describe either a point-like particle, or a more extended particle – the shape of which might be of interest itself. The boundaries of extended objects can optionally be delineated by first identifying particles and then applying a watershed segmentation seeded by those particles.[21] Whether shape is of interest or not, it is critical to first identify particles optimally. "Optimally" means that if the user had performed the identification manually, he/she would have defined the same set of particles as those found automatically. In Diatrack, this is achieved by interactively sliding the image analysis parameters values until the detection of particles (shown with crosses overlaid on top of the original images) cannot be improved further. In our experience, this brief but critical fine-tuning phase (which was also used to produce the results of the previous section) delivers better results compared to blind or to automated selection of image analysis parameters. In the remainder of this section, we briefly outline the successive steps of the tracking process.

Image pre-processing

In most instances, particle detection necessitates some preliminary pre-processing of the images. For example, the most efficient manner to detect candidate particles is to identify pixels that display an intensity higher than all their immediate neighbors ("Find particles" button in the control panel). If particles appear dark on a bright background, inverting the contrast is necessary ("Invert data" button …). An important pre-processing operation is Gaussian filtering, which smoothens out sharp image intensity variations corresponding to noise ("Filter data" …). Noise should be suppressed as much as possible but filtering should not alter significantly the lateral dimensions and visual appearance of objects. Another useful pre-processing operation is to subtract a local estimate of the background intensity ("Subtract background"…). In Diatrack, the background intensity is computed by filtering the image with a wide Gaussian kernel (i.e. we use the "Difference of Gaussians" method[22]). By trial and error, these few pre-processing operations suffice for most image sequences in order to subsequently produce an optimal set of particles.

Particle production

As mentioned, the workhorse object detector in Diatrack is the maximum intensity detector available from the control panel ("Find particles"). However, a range of other methods may also be accessed from the "Particle production" menu. For example, Diatrack offers a dedicated object detector for "in vitro motility assays", suited for filamentous objects (see Fig 3B).[23]

Particle selection

Only a minority of particles generated in the particle production phase corresponds to genuine objects. By using a combination of "Particle selection" tools from the control panel in an interactive manner, an optimal particle selection may be obtained. This is done e.g. by removing all particles featuring an intensity that is too dim or that are not sufficiently contrasted ("Remove… blurred"). Here, contrast is measured by dividing the intensity at the particle position by the average intensity around that particle.

Particle tracking

Once an optimal set of particles has been identified in the first image of the sequence, one may automatically process all remaining images using the currently selected parameters ("Process next frames"…). Diatrack can adaptively find the relevant particles in all frames even in the presence of photo-bleaching. Tracking per se can then be launched ("Track!" …) and all the trajectories are constructed and displayed. The only parameter required to be set for particle tracking is the maximum displacement amplitude (i.e. step size, expressed in pixels) that a particle can undergo between two successive images of the sequence. After tracking, it is advised to use the scrollbar of the control panel to step through the sequence. If particles have been tracked correctly, the spots that mark them should maintain their color over time. The Diatrack GUI provides all of the functionalities needed for manually correcting exceptional mistakes, but in our experience, a more productive path is to fine-tune the selected image analysis parameters to obtain yet better results.

Track selection and analysis

Not all trajectories are relevant for a particular type of analysis. For example, it is not recommended to compute diffusion coefficients or to quantify displacement effectiveness on very short-lived trajectories. Thus, a wide choice of trajectory selection tools is provided. In exceptional situations, the functionalities required to select and analyze tracks cannot be found within Diatrack. One may then save the entire Diatrack session ("File…Save current session…") and import the session file into Matlab™ where it can be analyzed further. For example, the x coordinate of the 5'th particle in the 70'th frame of the image sequence can be accessed by the expression: "tracks{70}.RefinedCooX(5)". The integrated intensity along that trajectory can then be computed by the Matlab snippet:

```
frame=70; part=5; IntSummed=0;

while(part)

IntSummed = IntSummed + tracks { frame }.Intensity(part) part =
tracks{ frame }.Successor(part);

frame = frame + 1;

end
```

where the "Successor" field of the array allows to follow particles along their respective trajectories. It would then be easy to select tracks on the basis of that integrated intensity criteria by setting the "Successor" field to zero for all undesirable tracks. Performing this type of analysis assumes some familiarity with the Matlab programming language.

Therefore, a wide range of track selection and analysis functions (over 50) are already available within the software.

Survey of applications

Tracking fluorescent speckles

Diatrack was originally developed to analyze fluorescent speckle microscopy (FSM) data.[9,24] In FSM, very low concentrations of fluorescently labeled actin or tubulin monomers are introduced into cells, where they incorporate into dynamic actin or microtubule networks. The statistical variations associated with this process are responsible for the production of small flecks of fluorescence, so called "speckles".[25] Speckles represent diffraction-limited regions of locally increased fluorophore concentration. Because the signal to noise ratio of speckles is very limited, and because speckles are present at high densities, it was a challenge to unambiguously identify and track them. In order to curb this complexity, the maximum amplitude of speckle jumps considered between successive frames was initially limited to 3 pixels and a nearest-neighbor approach was implemented.[26] Whereas a maximum jump amplitude of a few pixels represented a good value for the actin speckles that were tracked in the lamella of motile cells, those in their lamellipodium could undergo jumps of up to 10 pixels in amplitude at the relevant frame rate. Thus, for each speckle in a particular image frame, dozens of vicinal speckles from the next frame must be considered for correct trajectory assembly. Depending on the precise configuration of these speckles, trillions of possible assignments must be considered. Thus, a new approach was needed to compare and rank possible speckle assignments across multiple frames in a globally optimal manner. The Diatrack graph-based algorithm that we developed in this context has turned out exceptionally reliable.[27] It has also proved remarkably versatile as shown by the many applications beyond FSM, which we present next.

Tracking single molecules

Using modern optical microscopes, it has become possible to image and track signals corresponding to individual molecules. Diatrack was exploited for the first characterization of freely diffusing single proteins in buffer solution.[29] Under such conditions, molecules may undergo large jumps from image to image, which creates tracking ambiguities. In spite of this, diffusion coefficients within a few percent to those expected from the molecular masses and from Fluorescence Correlation Spectroscopy (FCS) measurements could be obtained for streptavidin and antibody fluorescent conjugates, as well as for quantum dots.

Several other studies of freely diffusing single molecules in 3D have been reported in more complex media. For example, Kappler *et al.* characterized the dynamics of single-molecules of hyaluronan in the microenvironment of human synovial fluid.[30] Grünwald et al probed the micro-environment within cell nuclei by microinjecting and tracking single molecules of fluorescent streptavidin conjugate.[31] In related experiments, single ribonucleoproteins were microinjected into cells and their dynamics and binding kinetics demonstrated the existence of preferential binding sites within nuclei.[32–34] English *et al.* were able to track single molecules of the fluorescent fusion protein RelA–Dendra2 within bacterial cells.[35,36] Using

a novel light sheet illumination setup, Ritter *et al.* used Diatrack to track single molecules deep within biological tissues.[37]

Diatrack was harnessed in single-molecule studies of the cell-penetrating HIV1 TAT peptide interacting with reconstituted vesicles by Ciobanasu *et al.*[38] In that case, single molecule diffusion primarily occurs within the two-dimensional (2D) environment of the vesicle bilayer. Ciobanasu *et al.* relied on the distribution of jump amplitude to determine diffusion coefficients; an approach that tends to be more robust than analyses based on mean square displacement measurements. Both distributions may be produced very easily in Diatrack. Using a similar approach, Kuzmenko et al. characterized the diffusion of Tom40 single proteins in the outer membrane of yeast mitochondria.[39–42]

Single-molecule diffusion and transport restricted to one dimension (1D) has been studied extensively.[43,44] This situation occurs often in biological imaging as molecular motors and enzymes can travel along cellular tracks afforded by microtubules, actin fibers, or DNA. This has provided for many exciting studies that have shed light on the mechanisms of molecular motors and enzymes. For example, Blainey *et al.* were able to measure diffusion and binding of the DNA repair enzyme hOgg1 along immobilized DNA strands in a flow chamber.[45] hOgg1 was labeled with a single molecule of the dye Cy3, and total internal reflection fluorescence microscopy together with Diatrack super-resolution spot tracking algorithm provided the necessary sensitivity to follow single enzymes with precision as good as 10 nanometers. Related studies include that of Lin *et al.* who studied the DNA repair enzyme C-Ada.[46] The same authors performed size-dependent diffusion studies to determine that certain enzymes actually spin around the DNA while undergoing 1D diffusion.[47] Other authors used antibody labeling of T7 RNA polymerase to measure the diffusion of this enzyme along stretched DNA, as well as the dependency of the interactions on the stretching force.[48]

Diatrack was used repeatedly to track beads attached at the extremity of single DNA strands immobilized in flow chambers. This experimental configuration has clarified the mechanisms underlying the activity of HIV-1 reverse transcriptase.[49] In this assay, the rate of reverse transcriptase activity correlates directly with sub-pixel shifts in bead position, as reverse transcriptase opens up DNA hairpin structures. The same setup was used by other researchers, including Park *et al.*, who also used FRET to measure DNA extension when the mismatch repair protein MutL binds DNA.[50–54]

In all these examples, the methodology to track single molecules is virtually identical. Because single molecules are small objects with a Gaussian-like (bell-shaped) intensity profile, one may detect them using local intensity maxima detection (default setting), followed by iterative Gaussian fitting. This will succeed, independently of whether the data is 2D or 3D (Diatrack will adapt to the circumstances automatically upon loading the data). A step by step visual tutorial for tracking Gaussian-like particles is provided under http://www.diatrack.org/subpixel.htm.

In vitro motility assays

The study of molecular motors such as myosin, kinesin, and dynein is greatly facilitated by in vitro motility assays (see Figure 3B). Here, motor proteins are immobilized on a surface and their motile activity is assessed by measuring the velocity of the cytoskeletal filaments they translocate (typically actin filaments or microtubules). Tracking actin filaments or microtubules requires careful image analysis because of their elongated geometry and flexible nature.

The automated tracking can become particularly difficult when low motor densities are used, as is the case in experiments to study motor processivity, i.e. the ability of a single molecular motor to productively interact with the filament without dissociating from it. In this context, investigators have regularly relied on Diatrack's dedicated functionalities for in vitro motility studies ('Particle production…' 'in vitro motility assay'). For example, Taft et al. demonstrated that myosin-5b is a processive motor[55] and Amrute-Nayak et al. succeeded in engineering single and double headed myosin-5 motors, whose mechanochemical properties (force, speed, processivity) could be systematically controlled by variations in ATP, ionic strength, and Mg^{2+}-ion concentrations[56]. Further, the effects of small molecules on myosins can be easily assessed in the in vitro motility assay by characterizing the changes in the velocity of filaments. Substances that specifically inhibit or activate myosins have been identified in e.g.[57–60]. Other in depth investigations of various myosins that exploited Diatrack include those of Weith, Diensthuber, and Chizhov.[34,58,61–65]

Clearly, tracking of elongated flexible polymers requires image analysis that differs from that which is appropriate for single molecules. Briefly, in order to segment crawling filaments, we use a form of edge detection guaranteeing the formation of closed contours in a pipeline described in detail in Vallotton *et al.*[66] Every detected connected region may then be retained or not on the basis of the average region intensity using the familiar GUI sliders.

Tracking membrane organelles and macromolecular complexes

Membrane vesicles are central to intracellular trafficking, acting as cargo containers that segregate, transport, and release their specific content to targeted organelles or subcellular regions. Their small spherical shape makes them ideal objects for Diatrack and their position and displacement can be pinpointed with great precision. Del Toro *et al.* first used Diatrack to characterize the trafficking of BDNF (Brain-derived neurotrophic factor), a peptide with polymorphisms implicated in Huntington's disease.[67] The software could also be used to detect and quantify the fusion of insulin-containing vesicles with the plasma membrane of beta cells under TIRF microscopy.[68] For this application, reliable tracking is paramount because track termination is used to pinpoint events of interest, such as vesicle fusions.[69,70] Kim et al. also tracked insulin vesicles and could uncover significant heterogeneity in their dynamics.[71,72] Trejo *et al.* tracked Na K-ATPase-containing vesicles in epithelial cells.[73] Pigment granules (melanosomes) could be tracked by Chang *et al.*[74] The motion of secretory granules during activation of neuroendocrine cells was characterized by Elias *et al.*[75] Other representative studies that investigated the motion of endosomes (see Figure 3F), ribonucleoprotein granules, telomeres, puncta and other protein clusters using Diatrack include those of Rai, Serpinskaya, Ling, Kim, Trelles-Sticken, Jacobs, and Bensenor.[76–82]

The tracking of vesicles and other organelles resembles that of single molecules insofar as they are small, compact objects. The main emphasis should be placed on determining an appropriate jump amplitude that is large enough to deal with even exceptionally long jumps. The value proposed by default by Diatrack represents only a very rough indication. Instead, the display should be made to switch periodically between any two frames of the sequence, and the largest jump should be visually identified and compared to the 10-pixel scale bar shown top left of the screen using the "Toggle" button of the GUI.

Tracking cells

Cells are very variable in their appearance—from coccal bacterial cells to star-like neurons. The best-case scenario in terms of tracking ease is when cells are round, with a core presenting higher intensities. In this case, Gaussian filtering followed by identification of local intensity maxima can locate the center of cells quite accurately. Cells that are expressing soluble cytosolic or nuclear fluorescent proteins are particularly convenient to track. Other contrasts may be suitable too. For example, Sakamoto *et al.* were able to use phase contrast microscopy to track tendon fibroblasts in a wound-healing assay that tested the ability of motile cells to fill a suddenly depleted area.[83] In many instances, it is possible to operate on the image contrast using dedicated image processing in order to obtain a single intensity maximum for each cell. For example, Abreu *et al.* used an image transform developed by Hadjidemtriou *et al.*[84] to identify mammary epithelial cells in bright-field images, followed by Diatrack processing.[85] Dedicated segmentation routines were also needed to reliably follow dense populations of bacilli in phase contrast images of expanding biofilms.[23] The pre-segmented images were then tracked using Diatrack ("Particle production"…"Pre-segmented") to generate tracks for each of thousands of bacteria (see Figure 3C).[66,86] This approach was used to examine the role of extracellular DNA (eDNA) in active biofilm expansion by *Pseudomonas aeruginosa*. These analyses revealed that eDNA enhances the frequency of individual cell movements. Diatrack can also locally average the motion of neighboring cells and generate flow movies describing dynamics at a coarse level. These movies show that the flow of cells through a biofilm is quite variable and reverses irregularly (See supplementary movie 2 and Inset of Figure 2C). Equipped with such tools, it will become easier to study cellular transport phenomena in biofilms.[66] Several other authors successfully used Diatrack as a cell tracker in 2D and 3D.[40,87,88]

Flows and mixing

In many applications, the interest is focused on the motion of the media for which the particles only act as a reporter. Such studies have a long history in fluid mechanics where the technique is known as particle image velocimetry (PIV). In PIV however, only a pair of images is typically acquired in short succession, and fluid motion information is obtained from computation of image correlation, rather than by particle tracking. Because it can precisely follow thousands of marker particles undergoing even large motions between successive images, Diatrack is particularly suited to study complex flow phenomena.

Diatrack allowed uncover the existence of converging flows of actin polymers in cell lamella, towards "depolymerization sinks" – foci where actin depolymerization is

preferentially taking place.[24] It also permitted for the first time to individually track and characterize the two antiparallel flows of tubulin that prevail in the mitotic spindle.[24]

Other complex flow phenomena have been elucidated using Diatrack. A particular example is the microscale flow in sessile drops and microchannels generated under nanometer amplitude high frequency surface vibration. The convoluted flow fields were characterized by Li *et al.*[89], Rogers *et al.*[90] and Dentry *et al.*[91] In the latter, the technique was used to show laminar to turbulent flow transition in acoustic streaming jets. The average rate of divergence of the trajectories of microparticles seeded within the acoustic streaming flow field could also be quantified (see Figure 3E), from which a Lyapunov exponent—a measure of the level of chaotic mixing in the system— was estimated.[92,93]

Other applications, including nanoparticle tracking and distance measurement

Being so small, nanoparticles typically appear as diffraction-limited spots under optical microscopy. In the presence of complex backgrounds, they may still be detected with excellent precision under dark field imaging. For example, Diatrack was used to measure the distance of silver nanoparticles from the cell wall of algae in 3D.[94] Diatrack has also been used several times in nano-manufacturing applications to precisely position gold nanoparticles on surfaces using optical traps.[95–99] Tracking of nanoparticles was also exploited by Liu *et al.* to monitor the motion of exoglucanases along cellulose fibers.[100] Tracking of functionalized quantum dots – another type of nanoparticles - as they penetrated cells and their nuclei was demonstrated by Kuo *et al.*[101]

Because Diatrack can pinpoint object coordinates with better than 0.01 pixel accuracy under optimal conditions, it is also well suited for nanometer distance measurements. Dange *et al.* used it to estimate the distance between the plane of the membrane bilayer and the binding site of the nuclear pore complex with accuracy better than 30 nm.[102,103] Analogously, distance measurements were performed between sites along single DNA polymers.[52] Another interesting application of this type consisted in measuring the displacement fields of dense polymeric nanopillar arrays to map cell traction forces.[104,105]

Conclusion and outlook

From the onset, Diatrack was developed as a particle tracking software rather than a general-purpose image analysis package. As a result, it has introduced and still offers one of the most complete sets of functions in this domain (see Table 1). Here, we showed that Diatrack 3.05 performs remarkably well across a wide range of tracking scenarios from the reference work of Chenouard *et al.*[19]

Over the years, Diatrack has supported many original research outcomes. The role of expert users is apparent from our survey and their contribution to the maturation of a tool such as Diatrack is impossible to overstate. With their help, Diatrack will continue to evolve for better interoperability, speed, and auditability. In our own laboratory, we are exploiting and further improving Diatrack specifically for tracking dim and highly dynamic mRNA particles during nuclear export – a demanding application for automated tracking technology (see Figure 3E).[106,107]

Future versions will make increased use of graphics processing unit capabilities and plugins will allow users to integrate routines developed by themselves. Several additional examples of applications in the form of detailed step-by-step tutorials are available on the website www.diatrack.org/Applications.html. There, it is shown how to track viral particles inside cells, how diffusion in colloid solutions may be measured, and how MRI magnetization grids can be tracked as a promising diagnostic tool for heart conditions. We hope to see yet many other applications in the future as we continue the development of the software.

Supplementary Material

Refer to Web version on PubMed Central for supplementary material.

Acknowledgments

References

1. Chudakov DM, Matz MV, Lukyanov S, Lukyanov KA. Fluorescent Proteins and Their Applications in Imaging Living Cells and Tissues. Physiological Reviews. 2010; 90(3):1103–1163. [PubMed: 20664080]

2. Toomre, D., Bewersdorf, JA. New Wave of Cellular Imaging. In: Schekman, R.Goldstein, L., Lehmann, R., editors. Annual Review of Cell and Developmental Biology Vol 26. Vol. 26. Palo Alto: 2010. p. 285-314.Annual Reviews

3. Meijering, E., Dzyubachyk, O., Smal, I. Methods for cell and particle tracking. In: Conn, PM., editor. Imaging and Spectroscopic Analysis of Living Cells: Optical and Spectroscopic Techniques. Vol. 504. San Diego: Elsevier Academic Press Inc; 2012. p. 183-200.

4. Manzo C, Garcia-Parajo MF. A review of progress in single particle tracking: from methods to biophysical insights. Rep Prog Phys. 2015; 78(12)

5. Reid D. An algorithm for tracking multiple targets. IEEE Trans Autom Control. 1979; 24(6):843–854.

6. Dalziel SB. Decay of Rotating Turbulence - Some Particle Tracking Experiments. Appl Sci Res. 1992; 49(3):217–244.

7. Saxton MJ, Jacobson K. Single-particle tracking: Applications to membrane dynamics. Annu Rev Bioph Biom. 1997; 26:373–399.

8. Sage D, Neumann FR, Hediger F, Gasser SM, Unser M. Automatic tracking of individual fluorescence particles: Application to the study of chromosome dynamics. Ieee T Image Process. 2005; 14(9):1372–1383.

9. Vallotton P. Quantitative analysis of time-lapse sequences. Bioworld. 2004; 1:2–3.

10. Vallotton P, Gupton SL, Waterman-Storer CM, Danuser G. Simultaneous mapping of filamentous actin flow and turnover in migrating cells by quantitative fluorescent speckle microscopy. P Natl Acad Sci USA. 2004; 101(26):9660–9665.

11. Vallotton P, Olivier S. Tri-track: Free Software for Large-Scale Particle Tracking. Microscopy and Microanalysis. 2013; 19(2):451–460. [PubMed: 23448973]

12. Matov A, Edvall MM, Yang G, Danuser G. Optimal-flow minimum-cost correspondence assignment in particle flow tracking. Computer Vision and Image Understanding. 2011; 115(4): 531–540. [PubMed: 21720496]

13. Yang, G., Matov, A., Danuser, G. Paper presented at: Proc of IEEE Computer Society Conference on Computer Vision and Pattern Recognition (CVPR). San Diego: 2005. Reliable Tracking of Large Scale Dense Antiparallel Particle Motion for Fluorescence Live Cell Imaging.

14. Padfield D, Rittscher J, Roysam B. Coupled minimum-cost flow cell tracking for high-throughput quantitative analysis. Medical Image Analysis. 2011; 15(4):650–668. [PubMed: 20864383]

15. Kuhn HW. The Hungarian Method for the assignment problem. Nav Res Log. 1955; 52(1):7–21.

16. Applegate KT, Besson S, Matov A, Bagonis MH, Jaqaman K, Danuser G. plusTipTracker: Quantitative image analysis software for the measurement of microtubule dynamics. J Struct Biol. 2011; 176(2):168–184. [PubMed: 21821130]

17. Thompson RE, Larson DR, Webb WW. Precise nanometer localization analysis for individual fluorescent probes. Biophys J. 2002; 82(5):2775–2783. [PubMed: 11964263]

18. Single-Molecule Localization Microscopy. http://bigwww.epfl.ch/smlm/software/_2016. http://bigwww.epfl.ch/smlm/software/

19. Chenouard N, Smal I, de Chaumont F, et al. Objective comparison of particle tracking methods. Nat Methods. 2014; 11(3):281–289. [PubMed: 24441936]

20. Crocker JC, Grier DG. Methods of Digital Video Microscopy for Colloidal Studies. *J.* Colloid Interface Sci. 1996; 179:298.

21. Soille P, Vincent L. Determining Watersheds in Digital Pictures Via Flooding Simulations. P Soc Photo-Opt Ins. 1990; 1360:240–250.

22. Lowe, DG. Object recognition from local scale-invariant features Computer Vision. Kerkyra, Greece: 1999.

23. Vallotton, P., Sun, C., Wang, D., Turnbull, L., Whitchurch, C., Ranganathan, P. Segmentation and tracking individual Pseudomonas aeruginosa bacteria in dense populations of motile cells; Paper presented at: 24th International Conference Image and Vision Computing; New Zealand. 2009.

24. Vallotton P, Ponti A, Waterman-Storer CM, Salmon ED, Danuser G. Recovery, visualization, and analysis of actin and tubulin polymer flow in live cells: a fluorescent speckle microscopy study. Biophys J. 2003; 85(2):1289–1306. [PubMed: 12885672]

25. Danuser G, Waterman-Storer CM. Quantitative fluorescent speckle microscopy: where it came from and where it is going. Journal of Microscopy-Oxford. 2003; 211:191–207.

26. Ponti A, Vallotton P, Salmon WC, Waterman-Storer CM, Danuser G. Computational analysis of F-actin turnover in cortical actin meshworks using fluorescent speckle microscopy. Biophys J. 2003; 84(5):3336–3352. [PubMed: 12719263]

27. Vallotton P, Small JV. Shifting views on the leading role of the lamellipodium in cell migration: speckle tracking revisited. Journal of Cell Science. 2009; 122(12):1955–1958. [PubMed: 19494123]

28. Walter NG, Huang C-Y, Manzo AJ, Sobhy MA. Do-it-yourself guide: how to use the modern single-molecule toolkit. Nat Methods. 2008; 5(6):475–489. [PubMed: 18511916]

29. Grunwald D, Hoekstra A, Dange T, Buschmann V, Kubitscheck U. Direct observation of single protein molecules in aqueous solution. Chemphyschem. 2006; 7(4):812–815. [PubMed: 16528778]

30. Kappler J, Kaminski TP, Gieselmann V, Kubitscheck U, Jerosch J. Single-molecule imaging of hyaluronan in human synovial fluid. Journal of Biomedical Optics. 2010; 15(6):060504–060504. [PubMed: 21198145]

31. Grunwald D, Martin RM, Buschmann V, et al. Probing intranuclear environments at the single-molecule level. Biophys J. 2008; 94(7):2847–2858. [PubMed: 18065482]

32. Grunwald D, Spottke B, Buschmann V, Kubitscheck U. Intranuclear binding kinetics and mobility of single native U1 snRNP particles in living cells. Molecular Biology of the Cell. 2006; 17(12):5017–5027. [PubMed: 16987963]

33. Siebrasse JP, Veith R, Dobay A, Leonhardt H, Daneholt B, Kubitscheck U. Discontinuous movement of mRNP particles in nucleoplasmic regions devoid of chromatin. P Natl Acad Sci USA. 2008; 105(51):20291–20296.

34. Weith AE, Previs MJ, Hoeprich GJ, et al. The extent of cardiac myosin binding protein-C phosphorylation modulates actomyosin function in a graded manner. Journal of Muscle Research and Cell Motility. 2012; 33(6):449–459. [PubMed: 22752314]

35. English BP, Hauryliuk V, Sanamrad A, Tankov S, Dekker NH, Elf J. Single-molecule investigations of the stringent response machinery in living bacterial cells. P Natl Acad Sci USA. 2011; 108(31):E365–E373.

36. Niu LL, Yu J. Investigating intracellular dynamics of FtsZ cytoskeleton with photoactivation single-molecule tracking. Biophys J. 2008; 95(4):2009–2016. [PubMed: 18390602]

37. Ritter JG, Veith R, Veenendaal A, Siebrasse JP, Kubitscheck U. Light Sheet Microscopy for Single Molecule Tracking in Living Tissue. Plos One. 2010; 5(7)

38. Ciobanasu C, Siebrasse JP, Kubitscheck U. Cell-Penetrating HIV1 TAT Peptides Can Generate Pores in Model Membranes. Biophys J. 2010; 99(1):153–162. [PubMed: 20655843]

39. Kuzmenko A, Tankov S, English BP, et al. Single molecule tracking fluorescence microscopy in mitochondria reveals highly dynamic but confined movement of Tom40. Scientific Reports. 2011; 1:195. [PubMed: 22355710]

40. Sieben A, Kaminski T, Kubitscheck U, Haberlein H. Terbutaline causes immobilization of single beta(2)-adrenergic receptor-ligand complexes in the plasma membrane of living A549 cells as revealed by single-molecule microscopy. Journal of Biomedical Optics. 2011; 16(2)

41. Mazerik JN, Kraft LJ, Kenworthy AK, Tyska MJ. Motor and Tail Homology 1 (TH1) Domains Antagonistically Control Myosin-1 Dynamics. Biophys J. 2014; 106(3):649–658. [PubMed: 24507605]

42. Mazerik JN, Tyska MJ. Myosin-1A Targets to Microvilli Using Multiple Membrane Binding Motifs in the Tail Homology 1 (TH1) Domain. Journal of Biological Chemistry. 2012; 287(16): 13104–13115. [PubMed: 22367206]

43. Lee AJ, Warshaw DM, Wallace SS. Insights into the glycosylase search for damage from single-molecule fluorescence microscopy. DNA Repair. 2014; 20:23–31. [PubMed: 24560296]

44. Schermerhorn KM, Tanner N, Kelman Z, Gardner AF. High-temperature single-molecule kinetic analysis of thermophilic archaeal MCM helicases. Nucleic Acids Res. 2016; 44(18):8764–8771. [PubMed: 27382065]

45. Blainey PC, van Oijent AM, Banerjee A, Verdine GL, Xie XS. A base-excision DNA-repair protein finds intrahelical lesion bases by fast sliding in contact with DNA. P Natl Acad Sci USA. 2006; 103(15):5752–5757.

46. Lin YH, Zhao T, Jian X, et al. Using the Bias from Flow to Elucidate Single DNA Repair Protein Sliding and Interactions with DNA. Biophys J. 2009; 96(5):1911–1917. [PubMed: 19254550]

47. Blainey PC, Luo GB, Kou SC, et al. Nonspecifically bound proteins spin while diffusing along DNA. Nature Structural & Molecular Biology. 2009; 16(12):1224–U1234.

48. Kim JH, Larson RG. Single-molecule analysis of 1D diffusion and transcription elongation of T7 RNA polymerase along individual stretched DNA molecules. Nucleic Acids Res. 2007; 35(11): 3848–3858. [PubMed: 17526520]

49. Kim S, Schroeder CM, Xie XS. Single-Molecule Study of DNA Polymerization Activity of HIV-1 Reverse Transcriptase on DNA Templates. Journal of Molecular Biology. 2010; 395(5):995–1006. [PubMed: 19968999]

50. Park J, Jeon Y, In D, Fishel R, Ban C, Lee JB. Single-Molecule Analysis Reveals the Kinetics and Physiological Relevance of MutL-ssDNA Binding. Plos One. 2010; 5(11)

51. Kath JE, Chang S, Scotland MK, et al. Exchange between Escherichia coli polymerases II and III on a processivity clamp. Nucleic Acids Res. 2016; 44(4):1681–1690. [PubMed: 26657641]

52. Tanner NA, Tolun G, Loparo JJ, et al. E. coli DNA replication in the absence of free beta clamps. Embo Journal. 2011; 30(9):1830–1840. [PubMed: 21441898]

53. Kath JE, Jergic S, Heltzel JMH, et al. Polymerase exchange on single DNA molecules reveals processivity clamp control of translesion synthesis. P Natl Acad Sci USA. 2014; 111(21):7647–7652.

54. Graziano V, Luo GB, Blainey PC, et al. Regulation of a Viral Proteinase by a Peptide and DNA in One-dimensional Space. Journal of Biological Chemistry. 2013; 288(3):2068–2080. [PubMed: 23043137]

55. Taft MH, Hartmann FK, Rump A, et al. Dictyostelium myosin-5b is a conditional processive motor. Journal of Biological Chemistry. 2008; 283(40):26902–26910. [PubMed: 18650439]

56. Amrute-Nayak M, Diensthuber RP, Steffen W, et al. Targeted Optimization of a Protein Nanomachine for Operation in Biohybrid Devices. Angew Chem-Int Edit. 2010; 49(2):312–316.

57. Chinthalapudi K, Taft MH, Martin R, et al. Mechanism and Specificity of Pentachloropseudilin-mediated Inhibition of Myosin Motor Activity. Journal of Biological Chemistry. 2011; 286(34): 29700–29708. [PubMed: 21680745]

58. Diensthuber RP, Muller M, Heissler SM, Taft MH, Chizhov I, Manstein DJ. Phalloidin perturbs the interaction of human non-muscle myosin isoforms 2A and 2C1 with F-actin. Febs Letters. 2011; 585(5):767–771. [PubMed: 21295570]

59. Fedorov R, Bohl M, Tsiavaliaris G, et al. The mechanism of pentabromopseudilin inhibition of myosin motor activity. Nature Structural & Molecular Biology. 2009; 16(1):80–88.

60. Radke MB, Taft MH, Stapel B, Hilfiker-Kleiner D, Preller M, Manstein DJ. Small molecule-mediated refolding and activation of myosin motor function. Elife. 2014; 3

61. Chizhov I, Hartmann FK, Hundt N, Tsiavaliaris G. Global Fit Analysis of Myosin-5b Motility Reveals Thermodynamics of Mg2+-Sensitive Acto-Myosin-ADP States. Plos One. 2013; 8(5)

62. Diensthuber RP, Tominaga M, Preller M, et al. Kinetic mechanism of Nicotiana tabacum myosin-11 defines a new type of a processive motor. Faseb J. 2014; 17:14–254763.

63. Heissler SM, Manstein DJ. Functional characterization of the human myosin-7a motor domain. Cellular and Molecular Life Sciences. 2012; 69(2):299–311. [PubMed: 21687988]

64. Heissler SM, Selvadurai J, Bond LM, et al. Kinetic properties and small-molecule inhibition of human myosin-6. Febs Letters. 2012; 586(19):3208–3214. [PubMed: 22884421]

65. Muller M, Diensthuber RP, Chizhov I, et al. Distinct Functional Interactions between Actin Isoforms and Nonsarcomeric Myosins. Plos One. 2013; 8(7)

66. Vallotton P. Size Matters: Filamentous Bacteria Drive Interstitial Vortex Formation and Colony Expansion in Paenibacillus vortex. Cytometry Part A. 2013; 83(12):1105–1112.

67. del Toro D, Canals JM, Gines S, Kojima M, Egea G, Alberch J. Mutant huntingtin impairs the post-Golgi trafficking of brain-derived neurotrophic factor but not its Val66Met polymorphism. Journal of Neuroscience. 2006; 26(49):12748–12757. [PubMed: 17151278]

68. Vallotton, P., James, DE., Hughes, WE. CMLS. Gold Coast, Queensland (Australia): 2007. Towards fully automated identification of vesicle-membrane fusion events in TIRF microscopy.

69. Lin CC, Huang CC, Lin KH, et al. Visualization of Rab3A dissociation during exocytosis: A study by total internal reflection microscopy. Journal of Cellular Physiology. 2007; 211(2):316–326. [PubMed: 17149709]

70. Gu Y, Huganir RL. Identification of the SNARE complex mediating the exocytosis of NMDA receptors. P Natl Acad Sci USA. 2016; 113(43):12280–12285.

71. Kim, HY., Jureller, JE., Kuznetsov, A., Philipson, LH., Scherer, NF. Quantifying local heterogeneity of in vivo transport dynamics using stochastic scanning multiphoton multifocal microscopy and segmented spatiotemporal image correlation spectroscopy. In: Periasamy, A., So, PTC., editors. Multiphoton Microscopy in the Biomedical Sciences Viii. Vol. 6860. Bellingham: Spie-Int Soc Optical Engineering; 2008.

72. Tabei SMA, Burov S, Kim HY, et al. Intracellular transport of insulin granules is a subordinated random walk. P Natl Acad Sci USA. 2013; 110(13):4911–4916.

73. Trejo HE, Lecuona E, Grillo D, et al. Role of kinesin light chain-2 of kinesin-1 in the traffic of Na,K-ATPase-containing vesicles in alveolar epithelial cells. Faseb Journal. 2010; 24(2):374–382. [PubMed: 19773350]

74. Chang L, Barlan K, Chou YH, et al. The dynamic properties of intermediate filaments during organelle transport. Journal of Cell Science. 2009; 122(16):2914–2923. [PubMed: 19638410]

75. Elias S, Delestre C, Ory S, et al. Chromogranin A Induces the Biogenesis of Granules with Calcium- and Actin-Dependent Dynamics and Exocytosis in Constitutively Secreting Cells. Endocrinology. 2012; 153(9):4444–4456. [PubMed: 22851679]

76. Rai A, Nothe H, Tzvetkov N, Korenbaum E, Manstein DJ. Dictyostelium dynamin B modulates cytoskeletal structures and membranous organelles. Cellular and Molecular Life Sciences. 2011; 68(16):2751–2767. [PubMed: 21086149]

77. Serpinskaya AS, Tuphile K, Rabinow L, Gelfand VI. Protein kinase Darkener of apricot and its substrate EF1 gamma regulate organelle transport along microtubules. Journal of Cell Science. 2014; 127(1):33–39. [PubMed: 24163433]

78. Ling SC, Fahrner PS, Greenough WT, Gelfand VI. Transport of Drosophila fragile X rental retardation protein-containing ribonucleoprotein granules by kinesin-1 and cytoplasmic dynein. P Natl Acad Sci USA. 2004; 101(50):17428–17433.

79. Kim H, Ling SC, Rogers GC, et al. Microtubule binding by dynactin is required for microtubule organization but not cargo transport. Journal of Cell Biology. 2007; 176(5):641–651. [PubMed: 17325206]

80. Trelles-Sticken E, Adelfalk C, Loidl J, Scherthan H. Meiotic telomere clustering requires actin for its formation and cohesin for its resolution. Journal of Cell Biology. 2005; 170(2):213–223. [PubMed: 16027219]

81. Jacobs DT, Weigert R, Grode KD, Donaldson JG, Cheney RE. Myosin Vc Is a Molecular Motor That Functions in Secretory Granule Trafficking. Molecular Biology of the Cell. 2009; 20(21): 4471–4488. [PubMed: 19741097]

82. Bensenor LB, Barlan K, Rice SE, Fehon RG, Gelfand VI. Microtubule-mediated transport of the tumor-suppressor protein Merlin and its mutants. P Natl Acad Sci USA. 2010; 107(16):7311–7316.

83. Sakamoto K, Owada Y, Shikama Y, et al. Involvement of Na+/Ca2+exchanger in migration and contraction of rat cultured tendon fibroblasts. Journal of Physiology-London. 2009; 587(22):5345–5359.

84. Hadjidemetriou S, Gabrielli B, Pike T, Stevens F, Mele K, Vallotton P. Detection and tracking of cell divisions in phase contrast video microscopy. Paper presented at: Third MICCAI Worshop on Microscopic Image Analysis with Applications in Biology. 2008

85. Abreu MTH, Hughes WE, Mele K, et al. Gab2 regulates cytoskeletal organization and migration of mammary epithelial cells by modulating RhoA activation. Molecular Biology of the Cell. 2011; 22(1):105–116. [PubMed: 21118992]

86. Gloag ES, Turnbull L, Huang A, et al. Self-organization of bacterial biofilms is facilitated by extracellular DNA. P Natl Acad Sci USA. 2013; 110(28):11541–11546.

87. Foolen J, Shiu JY, Mitsi M, Zhang Y, Chen CS, Vogel V. Full-Length Fibronectin Drives Fibroblast Accumulation at the Surface of Collagen Microtissues during Cell-Induced Tissue Morphogenesis. Plos One. 2016; 11(10)

88. Straub A, Krajewski S, Hohmann JD, et al. Evidence of Platelet Activation at Medically Used Hypothermia and Mechanistic Data Indicating ADP as a Key Mediator and Therapeutic Target. Arterioscl Throm Vas. 2011; 31(7):1607–U1317.

89. Li H, Friend JR, Yeo LY. Surface acoustic wave concentration of particle and bioparticle suspensions. Biomedical Microdevices. 2007; 9(5):647–656. [PubMed: 17530412]

90. Rogers PR, Friend JR, Yeo LY. Exploitation of surface acoustic waves to drive size-dependent microparticle concentration within a droplet. Lab on a Chip. 2010; 10(21):2979–2985. [PubMed: 20737070]

91. Dentry MB, Yeo LY, Friend JR. Frequency effects on the scale and behavior of acoustic streaming. Physical Review E. 2014; 89(1)

92. Shilton R, Tan MK, Yeo LY, Friend JR. Particle concentration and mixing in microdrops driven by focused surface acoustic waves. Journal of Applied Physics. 2008; 104(1)

93. Burov S, Tabei SMA, Huynh T, et al. Distribution of directional change as a signature of complex dynamics. P Natl Acad Sci USA. 2013; 110(49):19689–19694.

94. Vallotton P, Angel B, Mccall M, Kirby J. Imaging nanoparticle-algae interactions in three dimensions using Cytoviva microscopy. Journal of Microscopy. 2015; 257(2):166–169. [PubMed: 25421539]

95. Guffey MJ, Scherer NF. All-Optical Patterning of Au Nanoparticles on Surfaces Using Optical Traps. Nano Letters. 2010; 10(11):4302–4308. [PubMed: 20925400]

96. Yan ZJ, Shah RA, Chado G, Gray SK, Pelton M, Scherer NF. Guiding Spatial Arrangements of Silver Nanoparticles by Optical Binding Interactions in Shaped Light Fields. Acs Nano. 2013; 7(2):1790–1802. [PubMed: 23363451]

97. Yan ZJ, Manna U, Qin W, Camire A, Guyot-Sionnest P, Scherer NF. Hierarchical Photonic Synthesis of Hybrid Nanoparticle Assemblies. Journal of Physical Chemistry Letters. 2013; 4(16): 2630–2636.

98. Farniya AA, Esplandiu MJ, Bachtold A. Sequential Tasks Performed by catalytic pumps for colloidal crystallisation. Langmuir. 2014; 30(39):11841–11845. [PubMed: 25198923]

99. Yan ZJ, Gray SK, Scherer NF. Potential energy surfaces and reaction pathways for light-mediated self-organization of metal nanoparticle clusters. Nature Communications. 2014; 5

100. Liu YS, Zeng Y, Luo Y, et al. Does the cellulose-binding module move on the cellulose surface? Cellulose. 2009; 16:587–597.

101. Kuo CW, Chueh DY, Singh N, Chien FC, Chen PL. Targeted Nuclear Delivery using Peptide-Coated Quantum Dots. Bioconjugate Chemistry. 2011; 22(6):1073–1080. [PubMed: 21528926]

102. Dange T, Grunwald D, Grunwald A, Peters R, Kubitscheck U. Autonomy and robustness of translocation through the nuclear pore complex: a single-molecule study. Journal of Cell Biology. 2008; 183(1):77–86. [PubMed: 18824568]

103. Vallotton P. Differential aberration correction (DAC) microscopy: a new molecular ruler. Journal of Microscopy. 2008; 232(2):235–239. [PubMed: 19017222]

104. Kuo CW, Shiu JY, Chien FC, Tsai SM, Chueh DY, Chen PL. Polymeric nanopillar arrays for cell traction force measurements. Electrophoresis. 2010; 31(18):3152–3158. [PubMed: 20803755]

105. Khoo TF, Dang DH, Friend J, Oetomo D, Yeo L. Triple Degree-of-Freedom Piezoelectric Ultrasonic Micromotor via Flexural-Axial Coupled Vibration. Ieee Transactions on Ultrasonics Ferroelectrics and Frequency Control. 2009; 56(8):1716–1724.

106. Smith C, Lari A, Derrer CP, et al. In vivo single-particle imaging of nuclear mRNA export in budding yeast demonstrates an essential role for Mex67p. The Journal of cell biology. 2015; 211(6):1121–1130. [PubMed: 26694837]

107. Katz ZB, English BP, Lionnet T, et al. Mapping translation 'hot-spots' in live cells by tracking single molecules of mRNA and ribosomes. Elife. 2016; 5

108. Flores-Rodriguez N, Rogers SS, Kenwright DA, Waigh TA, Woodman PG, Allan VJ. Roles of Dynein and Dynactin in Early Endosome Dynamics Revealed Using Automated Tracking and Global Analysis. Plos One. 2011; 6(9)
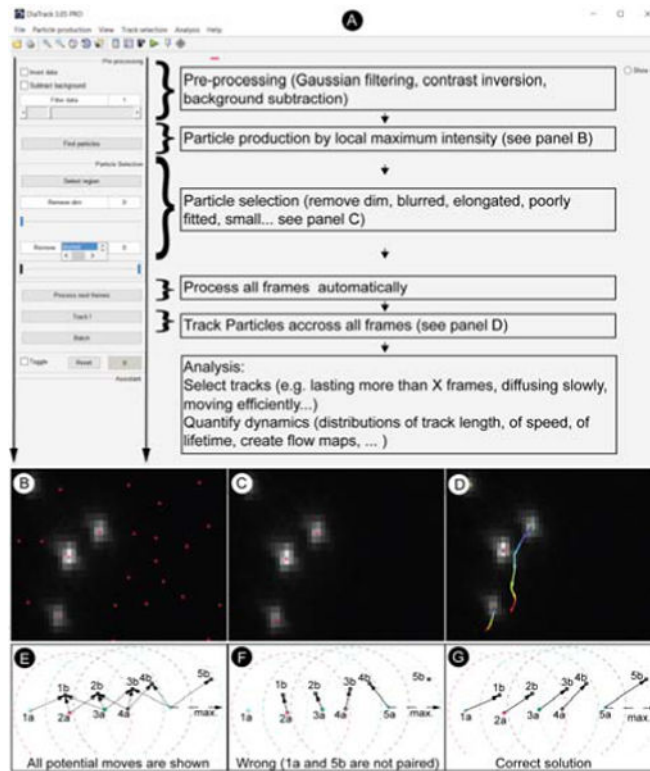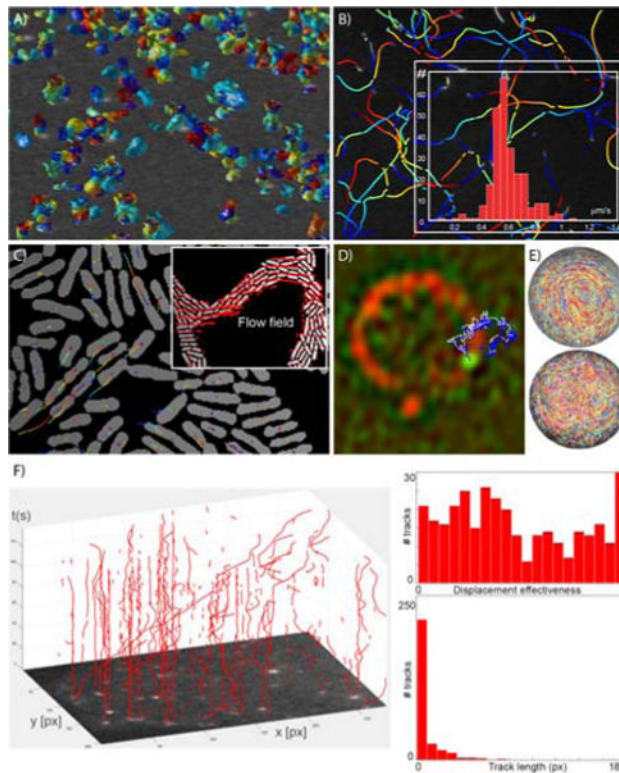
Figure 1.
A) The workflow in Diatrack guides the user naturally, from particle production (see panel B) and particle selection (see panel C), down to track production (see panel D), selection, and analysis. **B)** Immediately after particle production, a large number of particles do not correspond to genuine objects. **C)** Spurious particles must be systematically eliminated using a combination of selection tools such as the "remove blurred" slider, until only genuine particles are retained. **D)** The ability to identify and track spots with high precision even when they are in close proximity to each other is illustrated. A particle is seen passing near another one less than 3 pixels away. High precision tracking allows reporting on molecular events at the single-molecule level. **E)** Illustration of the notion of assignment conflict. In order to construct trajectories, particles 1a, 2a, 3a, 4a and 5a observed in time frame marked by "a" must be associated with particles seen at positions 1b, 2b, 3b, 4b and 5b one frame later. Given the maximum jump amplitude shown by dashed circles, all possible particle motions are indicated by dashed arrows. Particles compete with each other for assignment. **F)** In order to form tracks, one might first want to assign particle 3a with particle 2b because they lie in closest proximity. However, proceeding in order of proximity will eventually leave particle 1a and 5b unpaired (the suboptimal solution is shown). **G)** Using Diatrack's graph-based algorithm a solution that maximizes the pairing of particles may be found. Note that when particles are quite likely to disappear (e.g. in the presence of out of focus motion), the "suboptimal" solution shown in F) should probably be preferred over the "optimal solution" because the latter imposes a much greater total overall particle displacement. The best algorithm must strike a delicate balance between maximal matching of particles between frames and the ability to deal gracefully with particle appearance and disappearances (see Figure 2).
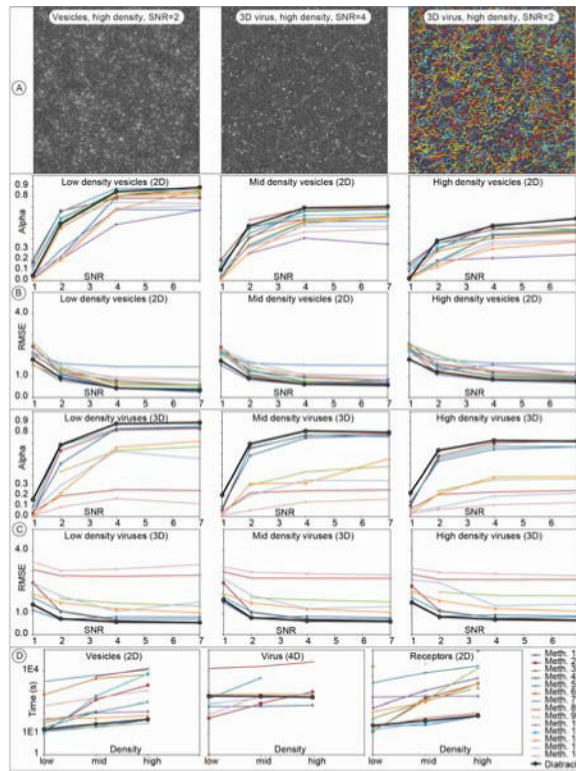
Figure 2. Tracking performance

The ground truth data from the work of Chenouard *et al.* were compared to the tracking results produced using Diatrack[19]. As described in Chenouard *et al.*, Alpha is a measure of track quality, while RMSE represents the root mean square discrepancy between true positions of particles and those corresponding positions found using Diatrack. The software performed really well, especially in light of the fact that it was not modified or tuned for the purpose of dealing with these particular data sets. It was also very fast in 2D (last row). Additional results may be found in the supplementary information.

Figure 3. Panel A) Example of 4D tracking
With the advances in computer performance, ever larger 4D data sets can be analyzed rapidly. Colored surfaces represent watershed-segmented objects and the tracks shown in red color connect the center of gravity of these surfaces over time. **B) Analysis of in vitro motility data.** Here, actin filaments were segmented using the "in vitro motility assay" particle production mode (time along tracks is color-coded from blue to red). The inset demonstrates in this situation a relatively narrow distribution of actin filament speed. **C) Diatrack can also track objects segmented by third party methods.** Here, bacteria were segmented as described in[23] and then tracked within our software using the "pre-segmented" mode. On the basis of this type of data, flow movies may be generated automatically that show locally coherent streaming of bacteria in the biofilm (see supplementary movie 2 and inset). **D) Automating identification of mRNA export events**. PP7-labelled mRNA particles (green channel) in yeast were tracked over time using both manual tracking (white trace), and using Diatrack (blue trace) -showing excellent overlap. Together with custom image analysis to detect the nuclear envelope (red channel), this high-throughput tool now routinely allows the identification of rare mRNA export events as well as their kinetic characterization (e.g. export time, nuclear envelope scanning time etc.). **E) Characterizing fluid flows.** Top view images of a planar cross-section of a liquid drop captured using a high-speed video camera. 5 μm fluorescent microparticles are observed to either follow smooth concentric trajectories associated with the acoustic streaming flow in a high viscosity drop (top), or exponentially divergent trajectories associated with chaotic acoustic streaming flow in a low viscosity drop (bottom). Each particle trajectory is labelled in a different color[92]. **F) Tracking GFP-Rab5 endosomes in RPE cells**. A subpopulation of these organelles is transported rapidly and efficiently along microtubules. In the

representation used here, time is coded as the vertical axis. The insets characterize the effectiveness of the displacements i.e. the ratio of straight-line trajectory length to total trajectory length, and the total track lengths, respectively. Original movie was obtained from Flores-Rodriguez et al.[108]

Table 1

Summary of main functionalities offered by Diatrack.

General features	Free	GUI-based, easy operation	Easy setup and standalone	Matlab compatible	Scripting support	Support for many proprietary image formats	Session storage and access to all internal variables
Tracking features	2D and 3D tracking	Super-resolution spot fitting in 2D and 3D	Watershed function	Manual editing of particles and tracks	Cell tracking	In vitro motility assay	Drift correction
Other features	Extensive track analysis functions	Extensive track selection options	Step by step application examples	Batch processing	Kymograph generation	Photo-bleaching correction	Particle counting